WILEY
Biotechnology and Bioengineering

Cascading effects in bioprocessing – The impact of mild hypothermia on CHO cell behaviour and host cell protein composition

Journal:	*Biotechnology and Bioengineering*
Manuscript ID	17-286.R1
Wiley - Manuscript type:	Article
Date Submitted by the Author:	n/a
Complete List of Authors:	Goey, Cher; Imperial College London, Chemical Engineering Tsang, Joshua; Imperial College London, Physics Bell, David; Imperial College London, Medicine Kontoravdi, Cleo; Imperial College London, Department of Chemical Engineering
Key Words:	Chinese hamster ovary cells, Quality by Design, mild hypothermia, apoptosis, host cell proteins

Cascading effect in bioprocessing – The impact of mild hypothermia on CHO cell behaviour and host cell protein composition

Cher H. Goey[1], Joshua M.H. Tsang[2], David Bell[3], Cleo Kontoravdi[1]

[1]Department of Chemical Engineering, Centre for Process Systems Engineering, Imperial College London, London SW7 2AZ, U.K.

[2]Department of Physics, Imperial College London, London SW7 2AZ, U.K.

[3]Department of Medicine, Imperial College London, London SW7 2AZ, U.K.

Abstract

A major challenge in downstream purification of monoclonal antibodies (mAb) is the removal of host cell proteins (HCPs). Previous studies have shown that cell culture decisions significantly impact the HCP content at harvest. However, it is currently unclear how process conditions affect physiological changes in the host cell population, and how these changes, in turn, cascade down to change the HCP profile. We examined how temperature downshift (TDS) to mild hypothermia affects key upstream performance indicators, i.e. antibody titre, HCP concentration and HCP species, across the cell culture decline phase and at harvest through the lens of changes in cellular behaviour. Mild hypothermic conditions introduced on day 5 of fed-batch Chinese hamster ovary (CHO) cell bioreactors resulted in a lower cell proliferation rate but larger percentages of healthier cells across the cell culture decline phase compared to bioreactors maintained at standard physiological temperature. Moreover, the onset of apoptosis was less evident in mild hypothermic cultures. Consequently, mild hypothermic cultures took an extra five days to reach an integral viable cell concentration (IVCC) and antibody yield similar to that of the control at standard physiological temperature. Despite having similar HCP concentration at harvest, mild hypothermic cell cultures reduced the variety of HCP species by 36%, including approximately 44% and 27% lower proteases and chaperones, respectively. This study suggests that TDS may be a good strategy to provide cleaner downstream feedstocks by reducing the variety of HCPs and to maintain product integrity by reducing the number of proteases and chaperones.

Keywords

Chinese hamster ovary cells; Quality by Design; mild hypothermia; apoptosis; host cell proteins

1. Introduction

One of the challenges identified in downstream purification (DSP) is HCP removal (Aboulaich et al., 2014; Levy et al., 2014; Sisodiya et al., 2012; Zhang et al., 2014). Apart from being potentially immunogenic for patients (Hanania et al., 2015; Ipsen, 2012), HCPs can cause product aggregation and fragmentation (Gao et al., 2011; Robert et al., 2009). For example, chaperones may interact with unfolded and partially folded recombinant proteins to form large aggregates, which cause fouling of chromatography columns and exchanger filters (Lintern et al., 2016). Proteases and glycosidases may cause mAb fragmentation and clipping in serum-free media, hence, reduce the overall product yield (Dorai and Ganguly, 2014; Gao et al., 2011). Therefore, efficient HCP removal is crucial to (1) ensure patient safety, (2) reduce DSP cost and (3) maintain product integrity.

Recent research has shown that cell culture conditions, such as harvest time and cell culture temperature, affect HCP composition in harvested cell culture fluid (HCCF) and in purified samples (Hogwood et al., 2013; Tait et al., 2013; Valente et al., 2015). For example, Valente et al. found that when CHO-K1 cells of different ages were cultured under the same conditions, they differentially expressed 92 HCPs, 34 of which have been reported as difficult to remove by purification, and 17 were strongly interacting with mAb. On the other hand, Tait et al. reported a 50% increase in HCP level of the HCCF of mild hypothermic culture compared to that of standard physiological temperature, which was due to accumulation of dead cells over a prolonged cell culture duration. These reports provide solid evidence of inseparable links between process conditions of upstream cell culture and HCP profile throughout the product capture and downstream purification train. This opens up the possibility to modify or reduce HCP composition by optimising upstream cell culture conditions under the Quality by Design (QbD) framework. However, there is an important

missing link: how do changes in process conditions alter the complex and dynamic host cell environment and, eventually, the make-up and abundance of HCPs in the supernatant?

In this study, the concept of QbD was implemented to understand the interplay between cell culture process conditions, CHO cell behaviour and extracellular HCP profile. The first step is to characterise the impact of cell culture temperature on a set of CHO cell responses, i.e. cell health and cell cycle distribution. According to Skindersoe and Kjaerulff (2014), apoptotic cell population exhibits low levels of reduced glutathione (GSH), which was designated as a biomarker in this study. The study continued by investigating the HCP composition in the culture supernatant at different culture time points and the corresponding cell viability. Identification of HCP species at harvest provided a useful database that will aid the optimisation of the design space towards producing an optimum downstream feedstock.

2. Materials and Methods

2.1. Cell line and cell culture system

Preparation of inoculums

GS-CHO 46 cell line expressing glutamine synthetase and cB72.3 chimeric IgG_4 antibody was kindly donated by Lonza Biologics. The cell line was revived and cultured in shake flasks (Corning, NY, USA) in CD CHO medium (Life Technologies, Paisley, UK) at 36.5°C in 8% of CO_2 humidified air, shaken at 140 rpm. Cells were subcultured in fresh medium every four days at a seeding density of 2 x 10^5 cells/mL and then transferred into the bioreactor on the fourth passage. The first and second passages were supplemented with 25μM L-Methionine Sulfoximine (MSX, Sigma-Aldrich, Dorset, UK).

Bioreactor operation

The 3L CellReady bioreactor (Applikon Biotechnology, Schiedam, the Netherlands) was inoculated at a seeding density of 3 x 10^5 cells/mL with an initial cell culture volume of 1.2L. The culture was mixed by an in-house up-pumping marine impeller rotating at 150 rpm and was supplied with a constant air flow rate of 22.5mL/min. The process was controlled with a *my-control* unit (Applikon Biotechnology, Schiedam, the Netherlands) at 36.5 ± 0.5°C with a heating blanket and pH 7.0 ± 0.1 with CO_2 supply and 100mM $NaHCO_3$/Na_2CO_3 alkali solution (Sigma-Aldrich, Dorset, UK). Dissolved oxygen tension (DOT) was set to a minimum of 50% with oxygen supply. These process parameters were monitored continuously with the BioExpert software version 1.1X (Applikon Technology, Schiedam, the Netherlands).

Cell cultures were supplemented with *CD EfficientFeed*^{TM} *C AGT*^{TM} (*Feed-C*, Life Technologies, Paisley, UK) at 10% cell culture volume on alternate days starting from day 2. Foaming was relieved with 5mL of 5% w/v of *Antifoam-C* (Sigma-Aldrich, Dorset, UK). Cell culture samples were collected daily and centrifuged at 800 rpm for 5 min. Aliquoted supernatants were stored at -80°C. The bioreactor working volume was kept within the range of 1L to 1.3L by drawing out excessive culture fluid every day after sampling and before any addition of *Feed-C* or *Antifoam-C*. For mild hypothermic experiments, cell culture temperature was reduced to 32.0 ± 0.5°C on day 5, corresponding to the late exponential cell growth phase, and maintained constant until harvest. All other process parameters were kept constant. Two bioreactor runs were conducted under each temperature regime.

2.2. Cellular behaviour

Cell count

Cell count was carried out with the trypan blue dye exclusion method and the *Viability and Cell Count* assay of the NucleoCounter® NC-250™ (ChemoMetec A/S, Allerod, Denmark) according to the manufacturer's instructions.

Cell cycle distribution

Total DNA content and cell cycle distribution of cell cultures were determined with the *2-Step Cell Cycle* assay of the NucleoCounter® NC-250™, and the results were visualised and analysed with the associated NucleoView software.

Cell health

Examination of cellular health was carried out with the *Vitality assay* of the NucleoCounter® NC-250™.

*All solutions (*Solution 18* for the *Cell Count* assay, *Solutions 10, 11* and *12* for the *2-Step Cell Cycle* assay and *Solution 6* for the *Vitality* assay) and slides for analyses with the NucleoCounter® NC-250™ were purchased from ChemoMetec A/S (Allerod, Denmark).

2.3. Analytical methods

Measurements of IgG_4 and extracellular metabolite concentrations

Extracellular IgG_4 concentration was measured with the BLItz system (Pall ForteBio Europe, Portsmouth, UK), which is a biolayer interferometry device. Extracellular concentrations of glucose (Glc), glutamate (Glu), glutamine (Gln), lactate (Lac) and ammonia (Amm) were quantified with the BioProfile 400 analyser (NOVA Biomedical, MA, USA).

Quantification of HCP concentration

HCP concentration in the cell culture supernatant was measured with a commercially available GS-HCP ELISA assay kit (Lonza Biologics, Slough, UK).

Identification of HCP species

HCP species in the cell culture supernatant were detected with liquid chromatography-mass spectrometry/mass spectrometry (LC-MS/MS). The protocol for sample preparation was adapted from the method described by Reisinger et al. (2014). Samples were filtered with 0.45µm syringe filters (VWR, Darmstadt, Germany). Then, 450µg of total protein were denatured in 4M guanidine HCl (Sigma-Aldrich, Dorset, UK) and reduced with 6.4mM dithiothreitol, DTT (Sigma-Aldrich, Dorset, UK) at 37°C for 1 hour. The sample was then alkylated with 13mM iodoacetamide (Sigma-Aldrich, Dorset, UK) in the dark at room temperature (around 20°C) for 1 hour. After that, the sample was quenched by adding 4.2mM DTT and buffer exchanged to 50mM, pH 8.0 Tris (Sigma-Aldrich, Dorset, UK) with 10K Microcon centrifugal filter devices (Merck Millipore, Cork, Ireland). MS-grade trypsin (Promega, WI, USA) was added with a mass ratio of 1µg of trypsin to 22µg of protein and left overnight at 37°C. Prepared samples were aliquoted and stored at -80°C until analysis.

Trypsin digested samples were analysed with an Infinity 1290 Binary LC system coupled to an iFunnel 6550 Quadrupole-Time-of-Flight liquid chromatography-mass spectrometer, QTOF LC-MS (Agilent Technologies, Santa Clara, CA). 20µL of the tryptic peptide sample was separated on a Zorbax Extend-C18 LC column, with 2.1 x 50mm dimensions and 1.8µm particle size (Agilent Technologies, Santa Clara, CA) by an 80-minutes gradient (solvent A: 0.1% formic acid in water; solvent B: 0.1% formic acid in acetonitrile). The following linear gradient was applied: 3-40% buffer B for 80 min, 40-90%

buffer B over 2 min then 100% buffer B over 2 min. Peptides were subjected to mass spectrometry (MS) and MS/MS as they eluted from the LC.

The data files acquired were extracted to generate peak lists, then submitted for database searches through the Spectrum Mill MS proteomic workbench, Rev B04.01.141 (Agilent Technologies, Santa Clara, CA). The spectra were searched against an in-house database of protein sequences of rodents (reviewed proteins of *Cricetulus griseus, Mesocricetus auratus, Mus musculus* and *Rattus norvegicus* downloaded from the UniProt website on 10-4-2015), IgG_4, and common contaminants like human keratins. Proteins identified with 95% confidence or greater were accepted.

3. Results and Discussion

3.1. Cell growth profile

Fed-batch cell cultures were grown in bioreactors until day 14 or when cell viability dropped below 80%, whichever came later. Industrial protocols typically use the 80% viability criterion for harvest. However, our study aimed to understand the correlation between cellular health and extracellular HCP profile, which could only be established if the data represented an extended culture duration. Figure 1(a) shows the cell growth profiles at standard physiological temperature and with a shift to mild hypothermia on day 5, corresponding to the late exponential cell growth phase. From Figure 1(a), cell growth profiles under the different conditions deviated on day 4 before converging again on day 5, even though conditions were the same and constant in all four bioreactors during the first five days of culture. Importantly, viable cell density was comparable across all four cultures on day 5 just before the TDS. At standard physiological temperature, cells grew exponentially from the start of the experiment and entered stationary phase on day 7. A maximum cell density of 1.5×10^7 cells/mL was achieved on day 7. On the other hand, upon induction of

TDS on day 5, cells entered an extended period of reduced cell growth until they reached a peak in cell density on day 9 (7.8 x 10^6 cell/mL). This was followed by a slow decline phase until day 14 in bioreactor *B-M1* and day 16 in bioreactor *B-M2*. This prolonged phase of low growth rate is a normal phenomenon of cell culture under mild hypothermia, which has been previously reported by Tait et al. (2013), Sou et al. (2015) and Yoon et al. (2006). Cultures grown under mild hypothermia displayed a maximum cell density 50% lower than that of the control and 40% reduction in the integral of viable cell concentration (IVCC) on day 14. Cells grown under mild hypothermia consumed glucose at a rate comparable to that of the control, while the specific lactate production rate was on average marginally higher under mild hypothermia (Figures S2 & S5). The specific glutamate consumption and glutamine production rates were comparable between the two temperatures (Figures S3 and S4), while the specific production rate of ammonia was higher under TDS up to day 8, switching to ammonia uptake from day 11 onwards.

3.2. Cell cycle distribution

Figure 1(b) shows the cell cycle distribution of cell cultures at standard physiological temperature and under mild hypothermia. For the control bioreactors, it is clear that the G_0/G_1 subpopulation gradually increased until day 6, after which the bioreactor duplicates, *B-S1* and *B-S2*, started to behave differently. The G_0/G_1 subpopulation in *B-S2* increased continuously until day 14, while that of *B-S1* decreased continuously. The loss in G_0/G_1 cells at late stage culture of *B-S1* coincided with the appearance of *sub-*G_0/G_1 cells from day 9 onwards (Figure S1c). This *sub-*G_0/G_1 cell population was determined with low DNA stainability and is believed to be caused by DNA fragmentation of apoptotic cells in *B-S1*. Previous studies by Al-Rubeai et al. (1995) and Gorczyca et al. (1992) support this claim by attributing the presence of *sub-*G_0/G_1 cells to an apoptotic cell population with fragmented DNA strands.

Interestingly, despite the different progression in the trend of G_0/G_1 distribution, the time profile of HCP/mAb ratio between the control duplicate remained unchanged (Figure S8). On the other hand, in mild hypothermic bioreactors, an additional 20% of cells immediately entered G_0/G_1 phase on day 6, one day after the TDS. This change appears to have been permanent with over 75% of cells remaining in G_0/G_1 phase until the end of cell culture period. The percentage of actively dividing cells was reduced from 37% on day 5 to approximately 16% from day 6 onwards (Figures S1a and S1b), resulting in a significantly lower cell growth, as shown in Figure 1(a). From Figure 1(b), it is interesting to observe that bioreactors *B-S2*, *B-M1* and *B-M2* showed a similar G_0/G_1 cell distribution from day 11 onwards, which indicates that cells had stopped proliferating in these runs. However, the halt in cell growth is believed to be caused by different factors in the bioreactors at standard physiological temperature compared to those under TDS: mild hypothermic cell cultures stopped growing due to cell arrest in G_0/G_1 phase from day 5 onwards (Figure 1b), while *B-S2* had high percentage of G_0/G_1 cells at late stage due to cell aging (Figure 3a, line) and depletion of glucose from day 10 onwards (Figures S7).

3.3. mAb titre and HCP concentration

Figure 2(a) shows the time profile of extracellular mAb titre of bioreactors at standard physiological temperature and under mild hypothermia. Up to day 5, the product titre between the two conditions was comparable. For the control bioreactors, mAb titre increased exponentially from day 5 to the end of cell culture. On the other hand, mAb production was significantly reduced under mild hypothermia. This is probably due to the significant reduction in cell density, as specific cell productivity (q_{mAb}) under mild hypothermia was averagely lower than at standard physiological temperature but not statistically different

(Figure S9). On day 14, mAb titre is approximately 60% higher in the control duplicate than in that with TDS.

At standard physiological temperature, the extracellular HCP concentration started to increase exponentially as early as day 7 and continued rising throughout the stationary phase (Figure 2b). From day 10 onwards, the concentration appeared to be increasing linearly although the changes were not statistically significant. The average value of HCP concentration after day 11 is 560 ± 63μg/mL. This observation is in good agreement with previous research by Hsu et al. (2012) and Yuk et al. (2015), who reported that HCP level reached a plateau at the end of the cell culture period in their systems. From Figure 2(b), mild hypothermic cell cultures contained low levels of HCPs until day 9. From day 10 onwards, HCP level started to rise but reached a significantly lower final concentration than the control bioreactors.

To elucidate the correlation between HCP content and cell viability, the percentage of dead cells across the cell culture period was superimposed onto the bar chart showing HCP concentration as a function of cell culture time, as shown in Figure 2(b). It is clear that the extracellular HCP concentration correlates well with the percentage of dead cells, suggesting that HCPs were released during the cell culture operation itself and not due to cell culture clarification, i.e. centrifugation.

Figure 2(b) also shows that the percentage of dead cells in the control bioreactors increased well above 10% from day 8 onwards, while the percentage of dead cells under mild hypothermic conditions was maintained below 10% until day 13 with low cell death rate observed for an extra six days post-TDS compared to the control bioreactors. This observation of reduced cell death under mild hypothermia is in good agreement with previous studies by Sou et al. (2014), Tait et al. (2013) and Trummer et al. (2006).

3.4. Cell health and HCP species

After the analysis of correlation between cell viability and extracellular HCP concentration, the next step was to understand the potential correlation between CHO cell health and the variety of HCP species across cell culture decline phase. To carry out this study, cell health was measured with the *Vitality assay* of the NucleoCounter-250, and HCP species present in the cell culture supernatants were identified with LC-MS/MS. With the *Vitality* assay, cell health was gauged by the level of reduced glutathione (GSH) stained with the fluorophore VitaBright-48™ (VB48). Cell subpopulations with low levels of reduced thiols were considered early apoptotic. The HCP profiles and early apoptotic cell density from day 8 to 14 were then observed together, as illustrated in Figures 3(a) and 3(b), while Figures 3(c) and 3(d) show the percentages of HCPs shared between the consecutive culture days.

From the results presented in Figure 3(a), significant numbers of intracellular HCPs and cell membrane proteins were detected as early as day 8 at standard physiological temperature, in the middle of the stationary phase when cell viability was still high (Figure 1a and Table S1). From day 8 to 12, the variety of intracellular HCPs and cell membrane proteins increased by 55 and 10 species, respectively. Interestingly, within this cell culture period, the percentage of apoptotic cells increased by nearly 2-fold (Figure 3a and Table S1). The last column in Table SI shows the total number of HCP species found in the supernatant up to day 14 of the cell cultures.

It is particularly noteworthy that the variety of intracellular HCPs was substantially reduced under mild hypothermic conditions (Figure 3b). From day 8 to 12, the numbers of intracellular HCPs and cell membrane proteins increased by 18 and four species, respectively, which were approximately 60% less than the rise in HCP profile across the same cell culture

duration of 36.5°C bioreactors. At the same time, as shown by the blue line in Figure 3(b), the apoptotic cell density did not exceed 10^5 cells/mL from day 8 to 12 under mild hypothermic conditions.

From the observation above, the increase in the number of HCP species and the corresponding apoptotic cell density appear to be closely related across the decline phase of cell cultures, as seen in Figures 3(a) and 3(b). At standard physiological temperature, the number of HCPs, especially those of intracellular nature, increased with apoptotic cell density. Following the same behavior, the variety of HCPs in mild hypothermic cultures was 60% lower in line with the reduced apoptotic cell population across the late stage of cell cultures.

Apoptosis is a controlled cell death process involving the activation of caspase-8 or caspase-9 pathways, which are known to alter the proteome of a cell (Schwamb et al., 2013; Wei et al., 2011), triggering the expression of many apoptosis-regulating HCPs as well as HCPs involved in DNA repair and cell death. Different morphological changes of apoptotic cells, including cell shrinkage and extensive cell membrane blebbing, as described by Ndozangue-Touriguine et al. (2008) and Stricker et al. (2010), would have contributed to the presence of many cell membrane proteins across the cell culture decline phase of the control bioreactors in this study (Figure 3a). In fact, the number of different cell membrane proteins found in the control bioreactor was double that observed under mild hypothermia (Figure 3b).

On the other hand, we hypothesise that secondary necrosis, an apoptotic cell death mechanism often observed in high-shear environments (Singh et al., 1994), took place on a greater scale in the control bioreactors. In these, late apoptotic cells became necrotic with degraded cytoplasmic fine structure and subsequently released a variety of intracellular HCPs into the cell culture medium, as illustrated by the high number of intracellular and cell

membrane proteins in 36.5°C decline phase in Figure 3(a). This was supported by the fact that apoptotic cells are the most shear-sensitive subset of cells according to Tait et al. (2013). They conducted shear stress test on a mixture of healthy and apoptotic cells and found that the apoptotic cell populations (both early and late apoptotic) were completely lost or significantly reduced after the shear tests.

Under both cell culture conditions, the number of naturally secreted proteins found in the supernatants across the cell culture decline phase was maintained (Figures 3a and 3b). Interestingly, from the *common* bars in Figures 3(c) and 3(d), the percentage of naturally secreted protein species commonly shared between different decline phases was consistently high. For instance, for the control bioreactors, 75% of naturally secreted HCP species were commonly shared between day 12 and 14. Similarly, approximately 72% of naturally secreted HCP species present on day 14 of the mild hypothermic samples were commonly shared with day 12. This suggests that these HCPs were secreted into the cell culture medium through the secretory pathways.

3.5. Antibody yield and HCP profile at theoretical harvest

To further understand the impact of upstream cell culture temperature on HCP composition in the supernatants prepared for downstream processing (i.e. downstream feedstocks), a theoretical harvest criterion was set to be the day when cell viability dropped below 80%. This criterion was achieved on day 9 and 11 for the control bioreactor duplicate and on day 14 and 16 for the mild hypothermic duplicate, even though in practice, the control bioreactors were not harvested until day 14. In the following sections, the term *harvest day* refers to these theoretical harvest time points for each bioreactor, and HCCF refers to the harvested cell culture fluid on these time points. A summary of cell culture performance indicators on these theoretical harvest days is presented in Table I.

At theoretical harvest time points, antibody yield was similar under both temperature conditions at 1.08 ± 0.15mg/mL at standard physiological temperature and 1.21 ± 0.15mg/mL with a shift to mild hypothermia (Table I). Moreover, the HCP concentration and HCP/mAb ratio were comparable between the two temperatures. The HCP concentrations were 355.8 ± 132.9µg/mL and 380.0 ± 166.2µg/mL, and the HCP/mAb ratios were 0.33 ± 0.13mg/mg and 0.31 ± 0.14mg/mg for the control and mild hypothermic cell cultures, respectively. Overall, at 80% cell viability, the quality of HCCF under both cell culture conditions was comparable with respect to these three indicators.

Venn diagram

To further understand if there was any difference in the quality of HCCF between the two conditions, the HCP species were sorted into three categories: (1) HCPs present in the HCCF of both the control and mild hypothermic bioreactors, (2) HCPs found only in the HCCF of the control bioreactors, and (3) HCPs found only in the HCCF of the mild hypothermic bioreactors, as shown in Figure 4. A total of 168 HCPs were found in both, 195 HCPs were unique to the control, and 63 HCPs were unique to mild hypothermic cell cultures. These corresponded to 46% and 27% of HCPs being unique to the upstream cell culture temperatures of 36.5°C and 32°C, respectively, showing that the HCP composition was significantly more diverse in the 36.5°C HCCF than in that of the 32°C bioreactors.

Subcellular locations

Figure 5 illustrates the number and proportion of HCP species found at the theoretical harvest time points, categorised according to their subcellular location that was assigned according to the description of these HCP species on the UniProt website. Under both cell culture conditions, over 65% of HCP species were intracellular, approximately 10% were

from the cell plasma membrane, and 13% were naturally secreted (Figure 5, pie charts). The impact of mild hypothermia on the proportion of HCP species in each subcellular location was not prominent. This HCP profile is in good agreement with Tait et al. (2012) who concluded that the majority of HCPs found in cell culture supernatants were intracellular. However, TDS substantially reduced the number of HCP species found in the HCCF (Figure 5, bar charts).

The *common* bars in Figure 5 show the number of HCP species present in the HCCF of both the control and mild hypothermic cell cultures. A comparison between the *32℃ harvest* bars and the *common* bars shows that a large proportion of the secreted and intracellular HCP pools in the HCCF of mild hypothermic bioreactors were also present in the HCCF of the control runs. Specifically, 79% of naturally secreted proteins and 72% of intracellular HCPs in the HCCF of mild hypothermic cell cultures were found to be in common with the control. Interestingly, cell membrane proteins found in the control and mild hypothermic HCCF were significantly different, and only 52% of the cell membrane components were shared between the two HCCF, indicating that nearly half of the cell membrane species in mild hypothermic HCCF were different from those in the control.

Baik et al. (2006), Kumar et al. (2008) and Underhill and Smales (2007) reported changes in the intracellular proteome of CHO cells under mild hypothermic conditions. Furthermore, Tait et al. (2013) found that the HCCF of mild hypothermic cell cultures is better clarified with lower solid particle retention and less loss in cell viability after centrifugation. They reasoned that CHO cells grown under mild hypothermic conditions are more shear-resistant as a result of homeoviscous adaptation of the cell membrane. Homeoviscous adaptation modifies the lipid composition of the cell membrane bilayer and, hence, activates specific signalling pathways (Roobol et al., 2011). Our results also suggest

that homeoviscous adaptation might have occurred to cells grown under mild hypothermic conditions, leading to modifications in cell membrane proteins. Nonetheless, this hypothesis requires further validations with more LC-MS/MS experiments on samples of cell pellets.

Primary functions

To further understand the impact of cell culture temperature on HCP composition of downstream feedstocks, HCPs found in the HCCF were categorised into 17 broad groups of primary cellular functions, as shown in Figure 6. This information was obtained from the UniProt website. Figure 6 shows that HCPs related to protein synthesis were the major group of HCP impurities present in HCCF, followed by metabolic enzymes and cytoskeletal proteins. This observation was consistent for both control and mild hypothermic cell cultures. TDS reduced the variety of HCPs in each primary functional group, especially HCPs involved in protein synthesis (- 0.41-fold), trafficking (- 0.65-fold), cellular response (- 0.5-fold) and component organisation (- 0.57-fold). This suggests that the HCCF of mild hypothermic cell cultures would be a better feedstock for Protein A purification, as HCPs related to protein synthesis, metabolism, cytoskeletal and chaperones are the main foulant of Protein A resins (Lintern et al., 2016). A summary of fold change in HCP variety upon TDS is provided in Table II.

Chaperones and proteolytic enzymes were found in the HCCF of bioreactors operated under both temperatures (Table II, HCP groups 10 and 12). Cell cultures at mild hypothermia reduced the variety of chaperones and proteases by 27% and 44%, respectively. TDS did not affect the presence of naturally secreted HCPs that possess folding or proteolytic capacities. Naturally secreted chaperones and proteases, i.e. *clusterin* and *serine protease HTRA1*, were present in the HCCF of both cell cultures. However, many intracellular and cell membrane proteins found in the HCCF of the controls were not found in that of mild hypothermic cell

cultures, including chaperones like the *heat shock proteins* and proteases like the *transmembrane protease serine 9* and *metalloprotease TIKI2*. This is hypothesised to be primarily due to the lower degree of cell lysis upon TDS. The next logical step in this analysis is to quantify the relative concentration of each of these species categories. This is because despite the reduction in HCP variety achieved under mild hypothermia, the overall concentration of HCPs at the theoretical harvest time points was comparable to that of the control bioreactors.

4. Conclusions

CHO cell culture operated with a shift to mild hypothermia in the late exponential cell growth phase sustained cell viability above 90% until the decline phase and suppressed apoptotic subpopulation below 2% throughout the cell culture period. As a result, the variety of HCPs at harvest, especially those of intracellular and cell membrane nature, was reduced. The counter-effect of TDS was repressed cell growth, which was accompanied by approximately 20% of actively dividing cells immediately entering G_0/G_1 phase upon TDS. Consequently, mild hypothermic cell cultures took an extra five days to reach an IVCC and IgG_4 yield similar to that of the cultures grown at standard physiological temperature, which coincided with the corresponding theoretical harvest day when cell viability dropped below 80%. Despite having similar HCP concentrations in the HCCF, the variety of HCP species was reduced by 36% under mild hypothermic conditions, including approximately 44% fewer protease and 27% fewer chaperone unique species. This is believed to be a result of sustained high cell viability and suppressed apoptotic cell population under mild hypothermia, which slowed down the expression of many HCPs related to apoptosis, cell repair and cell death. In summary, TDS did not enhance mAb titre and have prolonged the cell culture duration until the harvest criterion was met. Moreover, the typical CQAs of feedstocks for downstream

purification, i.e. mAb titre, HCP concentration and HCP/mAb ratio, were similar to that of the control. Nonetheless, the resulting HCCF from TDS cultures contained a significantly reduced variety of HCP species, including problematic proteases, chaperones and foulants of Protein A chromatography, and, hence, can be considered to be a better feedstock for downstream purification. Our work further shows that the definition of CQAs of feedstocks for downstream purification may require readjustment to include the variety of HCP species, especially proteins that possess catalytic or folding capacities, and known Protein A foulants identified by recent protein identification technologies like the LC-MS/MS.

Acknowledgements

CHG and CK would like to thank Karen Polizzi for her advice on HCP categorisation. CHG would like to thank the Department of Chemical Engineering, Imperial College London for her PhD scholarship.

Nomenclature

Amm	Ammonia
AO	Acridine orange
CHO	Chinese hamster ovary
CO_2	Carbon dioxide
DAPI	4',6-diamidino-2-phenylindole, dihydrochloride
DOT	Dissolved oxygen tension
DSP	Downstream processing
ELISA	Enzyme-linked immunosorbent assay
FDR	False discovery rate
FWHM	Full width at half maximum
Glc	Glucose
Gln	Glutamine
GS	Glutamine synthetase
GSH	Reduced glutathione
Glu	Glutamate
HCCF	Harvested cell culture fluid
HCP(s)	Host cell protein(s)
IgG(s)	Immunoglobulin G(s)
IVCC	Integral viable cell concentration
Lac	Lactate
LC-MS/MS	Liquid chromatography-mass spectrometry
mAb(s)	Monoclonal antibody (or antibodies)
MSX	L-Methionine sulfoximine
MW(s)	Molecular weight(s)
MWCO	Molecular weight cut-off
m/z	Mass to charge ratio
O_2	Oxygen
PBS	Phosphate buffer saline
PI	Propidium iodide
QbD	Quality by Design
q_{mAb}	Specific cell productivity
RPM	Revolutions per minute
RT	Retention time
TDS	Temperature downshift strategy
VB48	VitaBright-48^{TM}
vvm	Volume per volume per minute (gas volume flow per unit of liquid volume per minute)

References

Aboulaich N, Chung WK, Thompson JH, Larkin C, Robbins D, Zhu M. 2014. A novel approach to monitor clearance of host cell proteins associated with monoclonal antibodies. *Biotechnol Progr* **30**:1114–1124.

Al-Rubeai M, Singh RP, Goldman MH, Emery AN. 1995. Death mechanisms of animal cells in conditions of intensive agitation. *Biotechnol Bioeng* **45**:463–472.

Baik JY, Lee MS, An SR, Yoon SK, Joo EJ, Kim YH, Park HW, Lee GM. 2006. Initial transcriptome and proteome analyses of low culture temperature-induced expression in CHO cells producing erythropoietin. *Biotechnol Bioeng* **93**:361–371.

Dorai H, Ganguly S. 2014. Mammalian cell-produced therapeutic proteins: heterogeneity derived from protein degradation. *Curr. Opin. Biotechnol.* **30**:198–204.

Gao SX, Zhang Y, Stansberry-Perkins K, Buko A, Bai S, Nguyen V, Brader ML. 2011. Fragmentation of a highly purified monoclonal antibody attributed to residual CHO cell protease activity. *Biotechnol Bioeng* **108**:977–982.

Gorczyca W, Bruno S, Darzynkiewicz RJ. 1992. DNA strand breaks occurring during apoptosis: Their early in situ detection by the terminal deoxynucleotidyl transferase and nick translation assays and prevention by serine protease inhibitors. *International Journal of Oncology* **1**:639–648.

Hanania NA, Noonan M, Corren J, Korenblat P, Zheng Y, Fischer SK, Cheu M, Putnam WS, Murray E, Scheerens H, Holweg CT, Maciuca R, Gray S, Doyle R, McClintock D, Olsson J, Matthews JG, Yen K. 2015. Lebrikizumab in moderate-to-severe asthma: pooled data from two randomised placebo-controlled studies. *Thorax* **70**:748–756.

Hogwood CE, Bracewell DG, Smales CM. 2013. Host cell protein dynamics in recombinant CHO cells: impacts from harvest to purification and beyond. *Bioengineered* **4**:288–291.

Hsu W-T, Aulakh RPS, Traul DL, Yuk IH. 2012. Advanced microscale bioreactor system: a representative scale-down model for bench-top bioreactors. *Cytotechnology* **64**:667–678.

Ipsen. 2012. Ipsen's partner Inspiration Biopharmaceuticals announces hold of phase III clinical trials evaluating IB1001 for the treatment and prevention of Hemophilia B. Paris.

Kumar N, Gammell P, Meleady P, Henry M, Clynes M. 2008. Differential protein expression following low temperature culture of suspension CHO-K1 cells. *BMC Biotechnol* **8**:1–13.

Levy NE, Valente KN, Choe LH, Lee KH, Lenhoff AM. 2014. Identification and characterization of host cell protein product-associated impurities in monoclonal antibody bioprocessing. *Biotechnol Bioeng* **111**:904–912.

Lintern K, Pathak M, Smales CM, Howland K, Rathore A, Bracewell DG. 2016. Residual on column host cell protein analysis during lifetime studies of protein A chromatography. *J Chromatogr A* **1461**:70–77.

Ndozangue-Touriguine O, Hamelin J, Bréard J. 2008. Cytoskeleton and apoptosis. *Biochem Pharmacol* **76**:11–18.

Reisinger V, Toll H, Mayer RE, Visser J, Wolschin F. 2014. A mass spectrometry-based approach to host cell protein identification and its application in a comparability exercise. *Anal Biochem* **463**:1–6.

Robert F, Bierau H, Rossi M, Agugiaro D, Soranzo T, Broly H, Mitchell-Logean C. 2009. Degradation of an Fc-fusion recombinant protein by host cell proteases: Identification of a CHO cathepsin D protease. *Biotechnol Bioeng* **104**:1132–1141.

Roobol A, Roobol J, Carden MJ, Bastide A, Willis AE, Dunn WB, Goodacre R, Smales CM. 2011. ATR (ataxia telangiectasia mutated- and Rad3-related kinase) is activated by mild hypothermia in mammalian cells and subsequently activates p53. *Biochem J* **435**:499–508.

Schwamb S, Munteanu B, Meyer B, Hopf C, Hafner M, Wiedemann P. 2013. Monitoring CHO cell cultures: Cell stress and early apoptosis assessment by mass spectrometry. *J Biotechnol* **168**:452–461.

Singh RP, Al-Rubeai M, Gregory CD, Emery AN. 1994. Cell death in bioreactors: A role for apoptosis. *Biotechnol Bioeng* **44**:720–726.

Sisodiya VN, Lequieu J, Rodriguez M, McDonald P, Lazzareschi KP. 2012. Studying host cell protein interactions with monoclonal antibodies using high throughput protein A chromatography. *Biotechnol J* **7**:1233–1241.

Skindersoe ME, Kjaerulff S. 2014. Comparison of three thiol probes for determination of apoptosis-related changes in cellular redox status. *Cytometry A* **85**:179–187.

Sou SN, Sellick C, Lee K, Mason A, Kyriakopoulos S, Polizzi KM, Kontoravdi C. 2014. How does mild hypothermia affect monoclonal antibody glycosylation? *Biotechnol Bioeng* **112**:1165–1176.

Stricker J, Falzone T, Gardel ML. 2010. Mechanics of the F-actin cytoskeleton. *J Biomech* **43**:9–14.

Tait AS, Tarrant RDR, Velez-Suberbie ML, Spencer DIR, Bracewell DG. 2013. Differential response in downstream processing of CHO cells grown under mild hypothermic conditions. *Biotechnol Progr* **29**:688–696.

Trummer E, Fauland K, Seidinger S, Schriebl K, Lattenmayer C, Kunert R, Vorauer-Uhl K, Weik R, Borth N, Katinger H, Muller D. 2006. Process parameter shifting: Part I. Effect of DOT, pH, and temperature on the performance of Epo-Fc expressing CHO cells cultivated in controlled batch bioreactors. *Biotechnol Bioeng* **94**:1033–1044.

Underhill M, Smales CM. 2007. The cold-shock response in mammalian cells: investigating the HeLa cell cold-shock proteome. *Cytotechnology* **53**:47–53.

Valente KN, Lenhoff AM, Lee KH. 2015. Expression of difficult-to-remove host cell protein impurities during extended Chinese hamster ovary cell culture and their impact on continuous bioprocessing. *Biotechnol Bioeng* **112**:1232–1242.

Wei Y-YC, Naderi S, Meshram M, Budman H, Scharer JM, Ingalls BP, McConkey BJ. 2011. Proteomics analysis of Chinese Hamster Ovary cells undergoing apoptosis during prolonged cultivation. *Cytotechnology* **63**:663–677.

Yoon SK, Hong JK, Choo SH, Song JY, Park HW, Lee GM. 2006. Adaptation of Chinese hamster ovary cells to low culture temperature: Cell growth and recombinant protein production. *J Biotechnol* **122**:463–472.

Yuk IH, Nishihara J, Walker D, Huang E, Gunawan F, Subramanian J, Pynn AFJ, Yu XC, Zhu-Shimoni J, Vanderlaan M, Krawitz DC. 2015. More similar than different: Host cell protein production using three null CHO cell lines. *Biotechnol Bioeng* **112**:2068–2083.

Zhang Q, Goetze AM, Cui H, Wylie J, Trimble S. 2014. Comprehensive tracking of host cell proteins during monoclonal antibody purifications using mass spectrometry. *MAbs* **6**:659–670.

Tables

Table I Summary of bioreactor performance on theoretical harvest days

Performance indicators	Cell culture temperature	
	36.5°C	32°C from day 5
Harvest day	11 and 9	14 and 16
IVCC (10^6 cells.h/mL)	1774 ± 465	1743 ± 213
Cell viability (%)	71.1 ± 7.3	77.5 ± 2.1
Average cell specific productivity (pg/cell/h)	0.659 ± 0.165	0.636 ± 0.156
IgG_4 titre (mg/mL)	1.08 ± 0.15	1.21 ± 0.15
HCP concentration (µg/mL)	355.8 ± 132.9	380.0 ± 166.2
HCP/IgG_4 (mg/mg)	0.33 ± 0.13	0.31 ± 0.14

Table II Variety of HCP species in the HCCF of the control and mild hypothermic bioreactors grouped according to primary cellular function

Group	Primary cellular functions	Number of HCP species		
		36.5°C harvest	32°C harvest	Fold change
1	Protein synthesis	68	40	-0.41
2	Metabolism	40	31	-0.23
3	Cytoskeletal	38	28	-0.26
4	Protein modification	25	19	-0.24
5	Homeostasis	24	18	-0.25
6	Trafficking	23	8	-0.65
7	Signalling	20	14	-0.30
8	Cell cycle & growth	19	13	-0.32
9	Cellular response	18	9	-0.50
10	**Chaperone**	**15**	**11**	**-0.27**
11	Cell adhesion/migration	12	9	-0.25
12	**Proteolysis**	**9**	**5**	**-0.44**
13	Binding	11	5	-0.55
14	Component organisation	7	3	-0.57
15	Regulation	4	4	0.00
16	Histone	2	1	-0.50
17	Uncharacterised	28	13	-0.54
	Total HCP species	**363**	**231**	**-0.36**

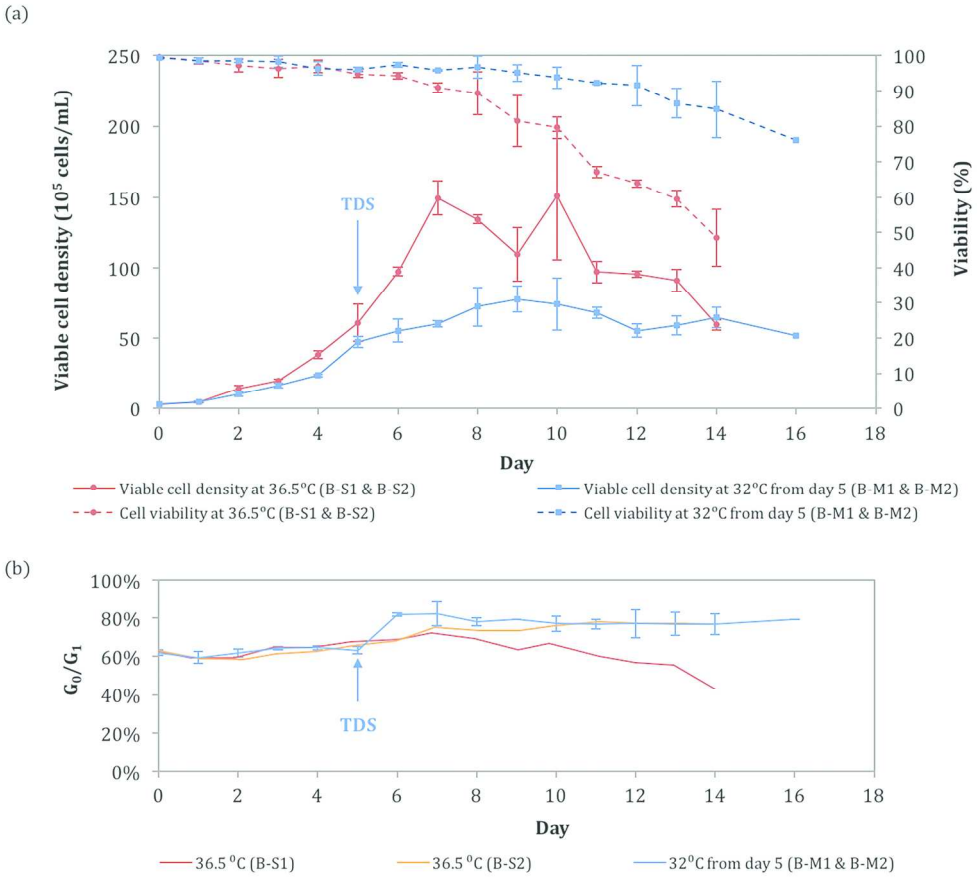

Figure 1. (a) Cell growth and cell viability and (b) percentage of cells in G0/G1 phase at standard physiological temperature (36.5°C) or with TDS to mild hypothermia (32°C) from day 5. Error bars are standard deviations of biological duplicate.

165x147mm (300 x 300 DPI)

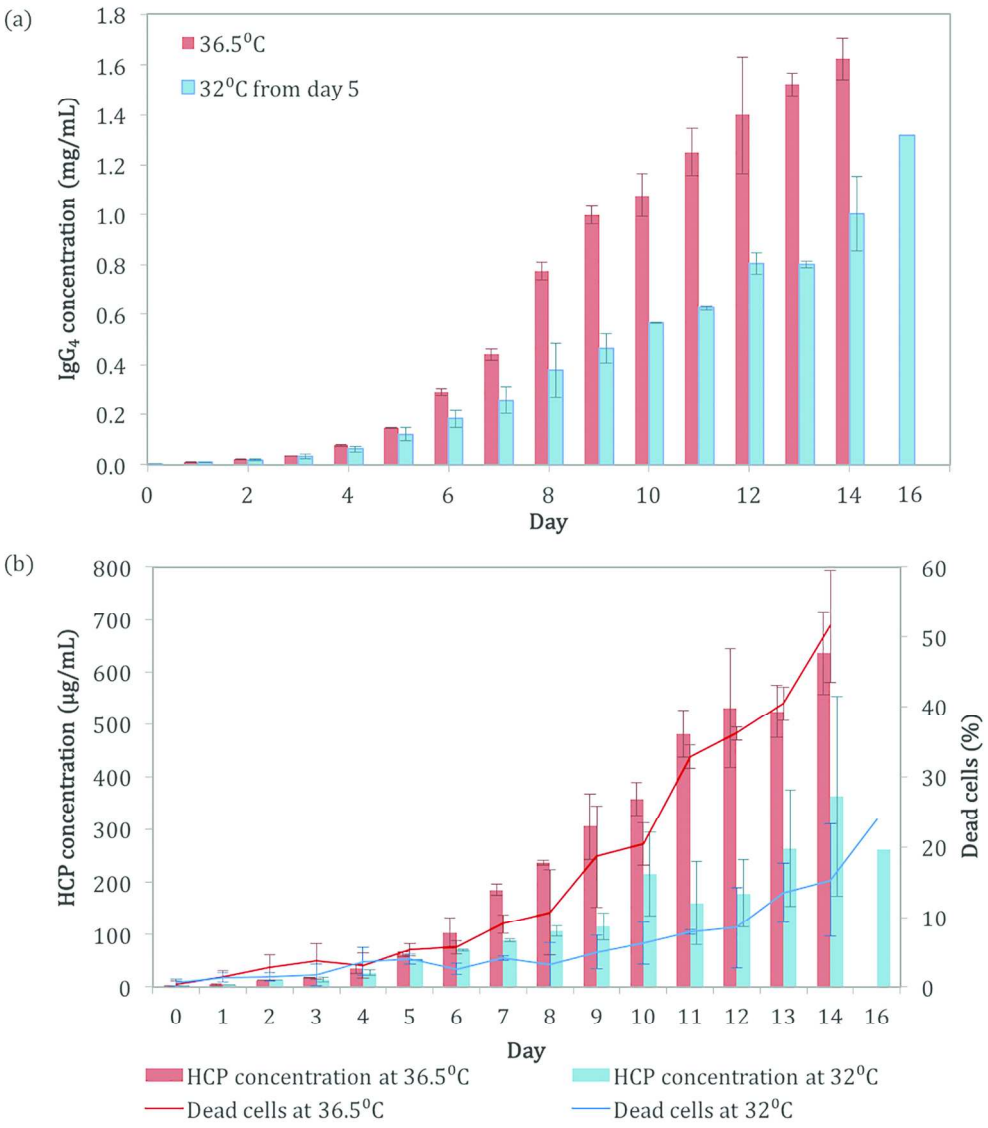

Figure 2. (a) IgG4 concentration and (b) HCP concentration and percentage of dead cells in the cell culture supernatants of bioreactors operated at standard physiological temperature (36.5°C) or with TDS to mild hypothermia (32°C) from day 5. Error bars of IgG4 concentration, HCP concentration and percentage dead cells are the respective standard deviations of biological duplicate. Measurements by BLItz and HCP ELISA kit were conducted in technical duplicate.

152x171mm (300 x 300 DPI)

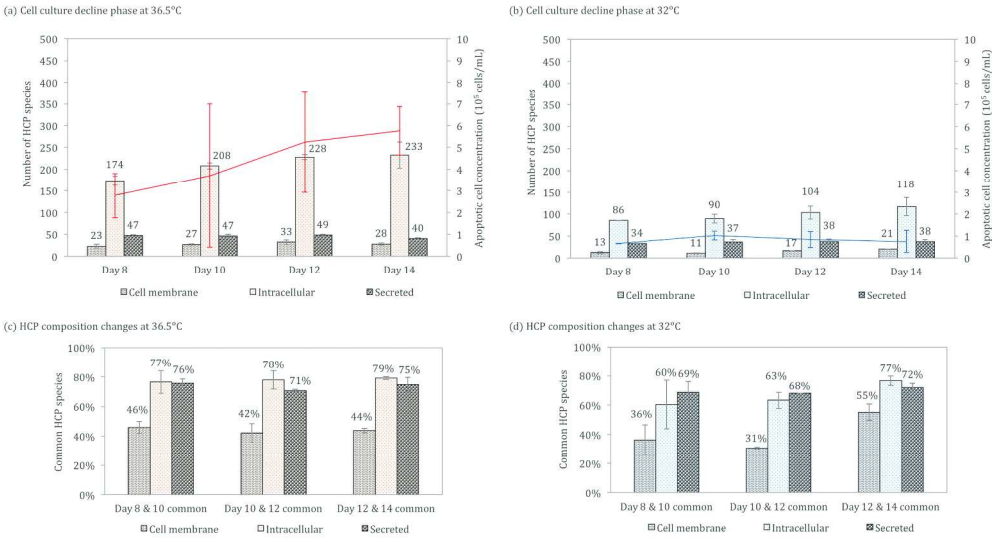

Figure 3. HCP profile across the cell culture decline phase: Bar charts illustrate the proportion of HCP species found across the bioreactor decline phase in terms of subcellular locations at (a) 36.5°C and (b) with a shift to 32°C from day 5. Lines show the corresponding concentration of apoptotic cells. The percentage of HCP species in common between neighbouring cell culture days at 36.5°C and 32°C is shown in Figures (c) and (d), respectively. Error bars represent standard deviation of duplicate bioreactor runs.

254x138mm (300 x 300 DPI)

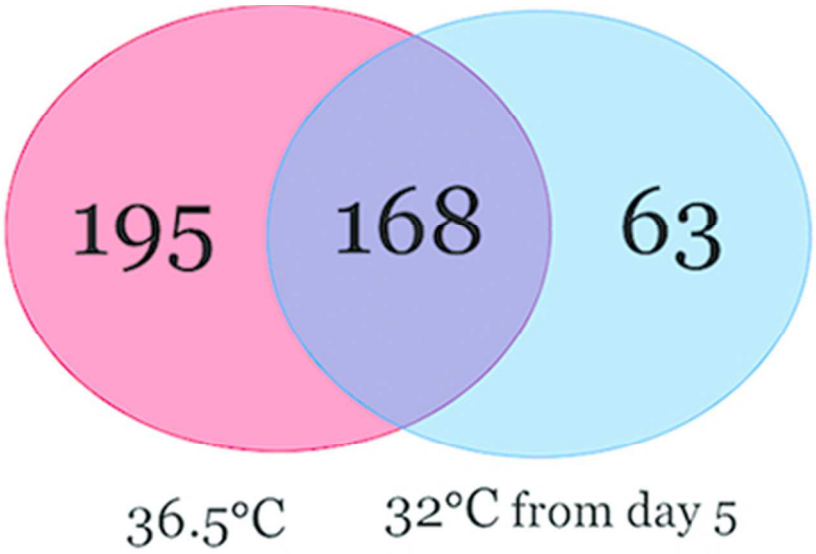

Figure 4. Number of HCP species found in HCCF samples of cell cultures at standard physiological temperature (red), under mild hypothermia (blue) and under both process conditions (overlapping area).

38x23mm (300 x 300 DPI)

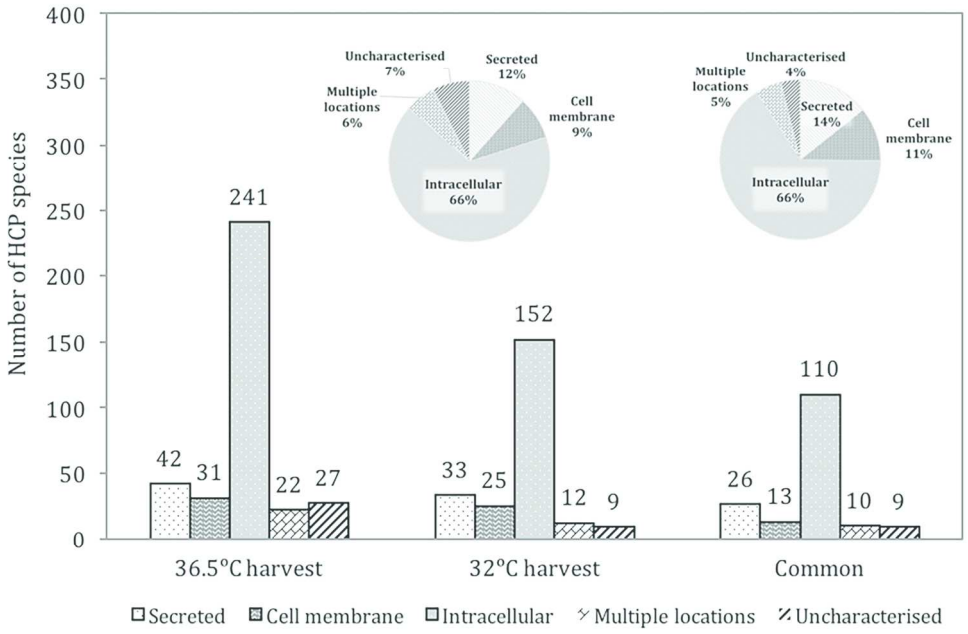

Figure 5. Secreted or lysed? Subcellular location of HCP species found in the HCCF of cell cultures conducted at 36.5°C and with a shift to 32°C from day 5. Pie charts show the proportion of HCP species in each subcellular location: 36.5°C on the left and 32°C from day 5 on the right.

152x101mm (300 x 300 DPI)

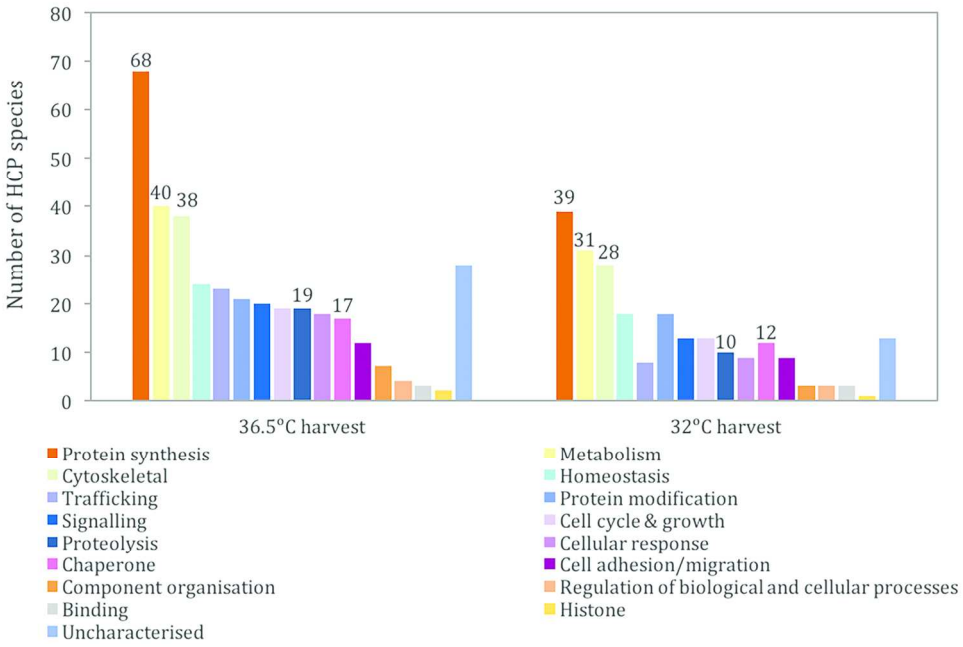

Figure 6. Primary cellular functions of HCPs in the HCCF of cell cultures conducted at 36.5°C and with a shift to 32°C from day 5, as described on the UniProt database.

152x98mm (300 x 300 DPI)

Supplementary Material

Cascading effect in bioprocessing – The impact of mild hypothermia on CHO cell behaviour and host cell protein composition

Cher H. Goey, Joshua M.H. Tsang, David Bell, Cleo Kontoravdi

Table S1: Summary of cell viability, apoptotic cell density and HCP profile across bioreactor decline phase at 36.5°C and 32°C from day 5.

Culture temperature	Culture day	Cell viability (%)	Apoptotic cell density (10^5 cells/mL)	HCP concentration (µg/mL)	HCP species
36.5°C	8	89.3 ± 6.1	2.8 ± 1.0	236.4 ± 4.2	244 ± 18
	10	79.6 ± 3.0	3.7 ± 3.3	357.4 ± 31.3	282 ± 5
	12	63.9 ± 0.9	5.2 ± 2.3	530.4 ± 113.0	309 ± 13
	14	48.5 ± 8.0	5.8 ± 1.1	636.2 ± 78.8	301 ± 30
32°C from day 5	8	96.8 ± 3.2	0.7 ± 0.0	106.5 ± 10.1	132 ± 4
	10	93.7 ± 3.0	1.0 ± 0.2	215.3 ± 79.5	138 ± 14
	12	91.5 ± 5.7	0.9 ± 0.4	178.9 ± 64.1	158 ± 8
	14	84.7 ± 8.0	0.8 ± 0.5	363.3 ± 189.8	176 ± 15

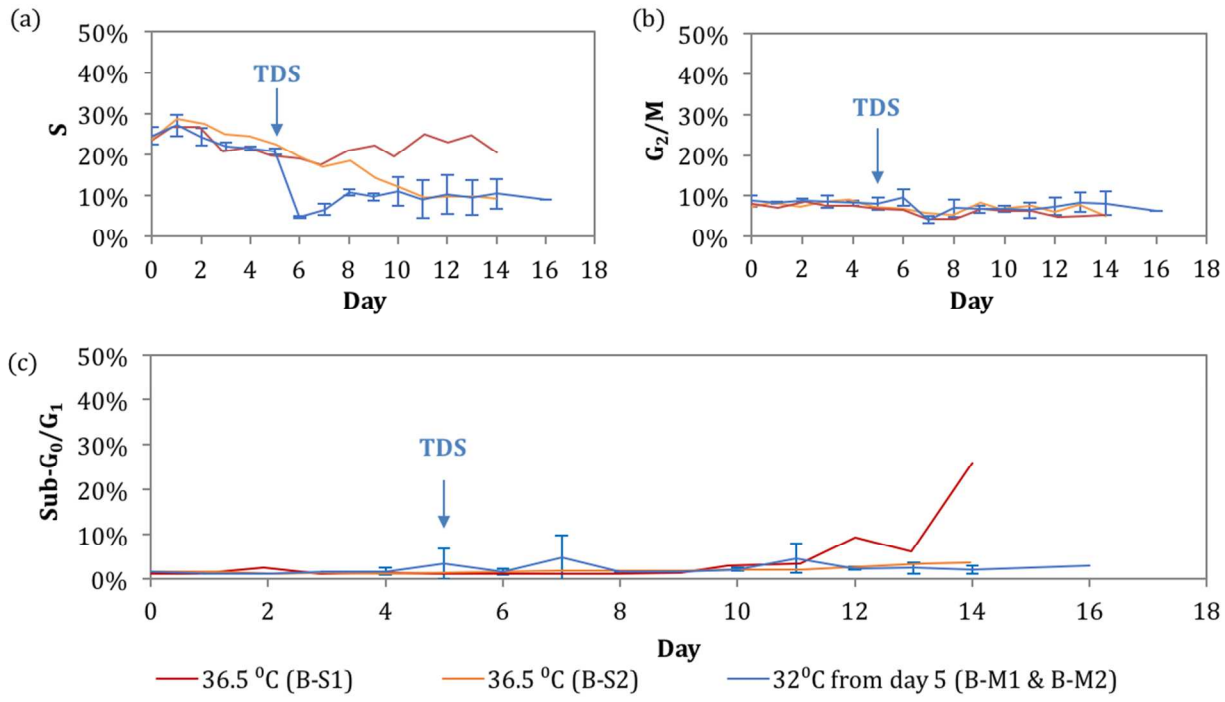

Figure S1: Cell cycle distribution: Percentage of cells in (a) synthetic *S* and (b) mitotic *G_2/M* phases and (c) *sub-G_0/G_1* phase. Error bars represent standard deviation of bioreactor duplicate.

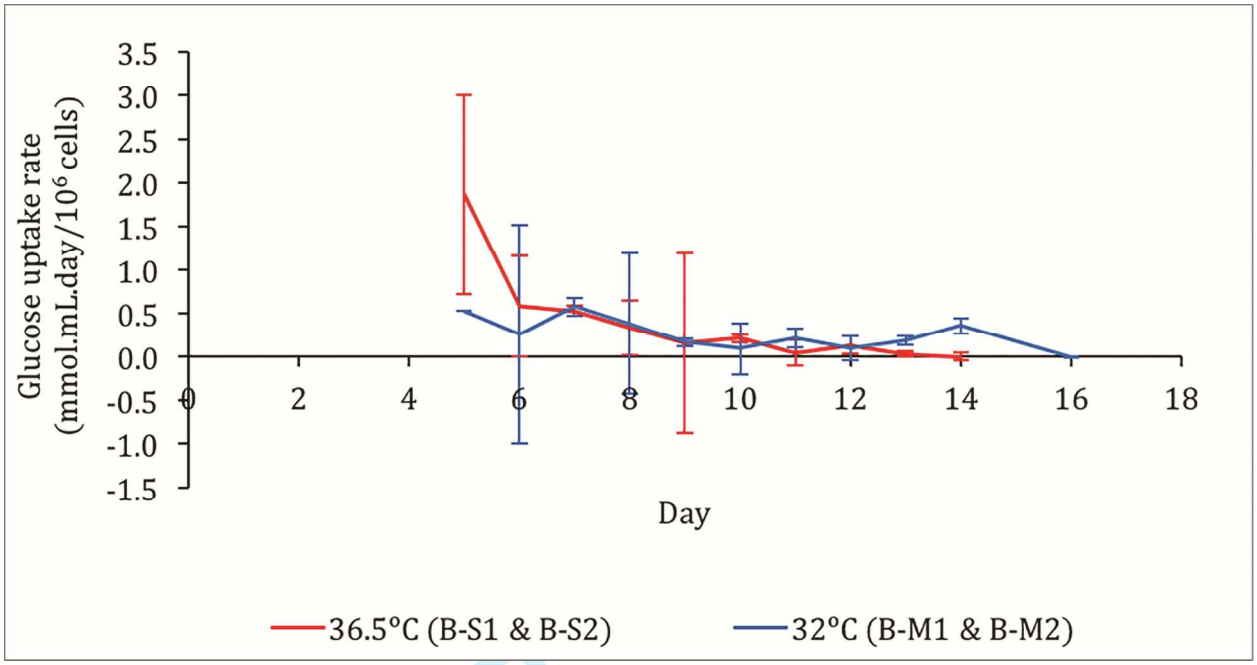

Figure S2: Specific glucose uptake rate at 36.5°C and 32°C from day 5.

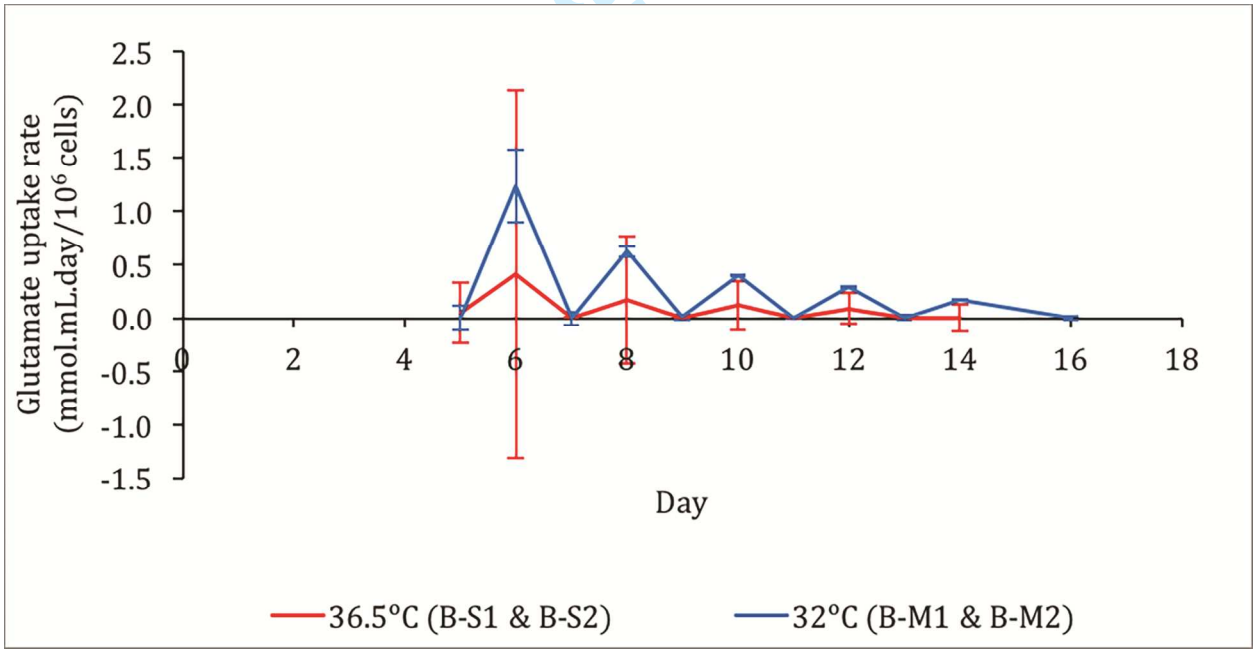

Figure S3: Specific glutamate uptake rate at 36.5°C and 32°C from day 5.

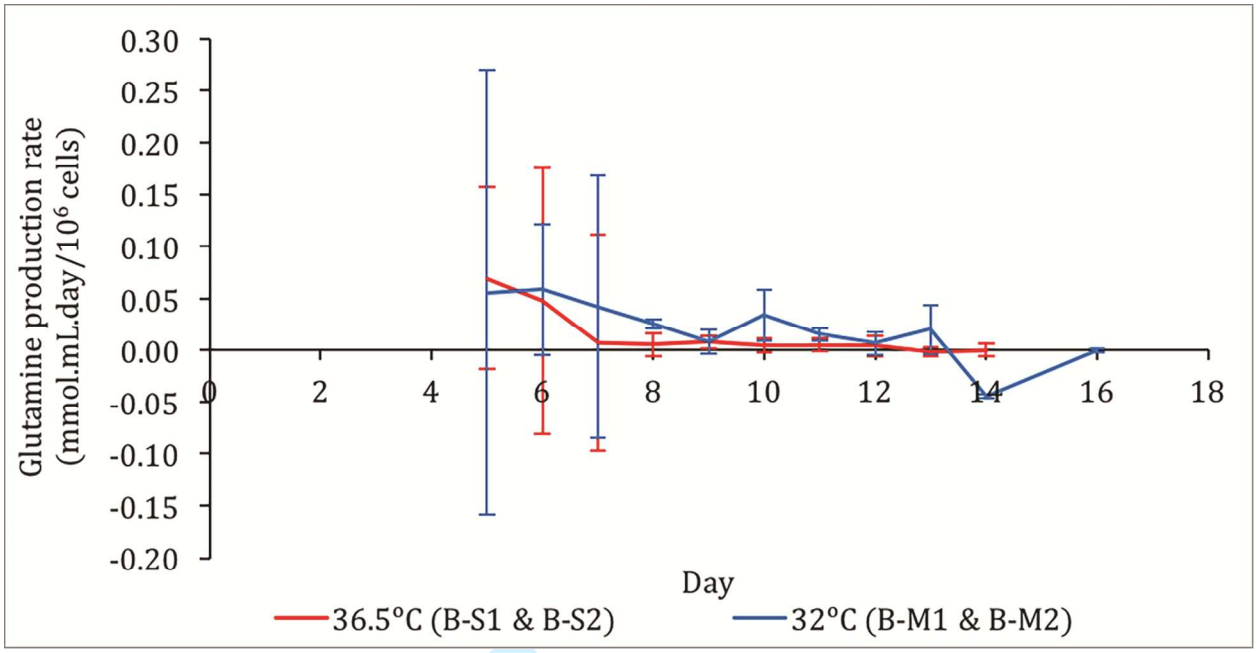

Figure S4: Specific glutamine production rate at 36.5°C and 32°C from day 5.

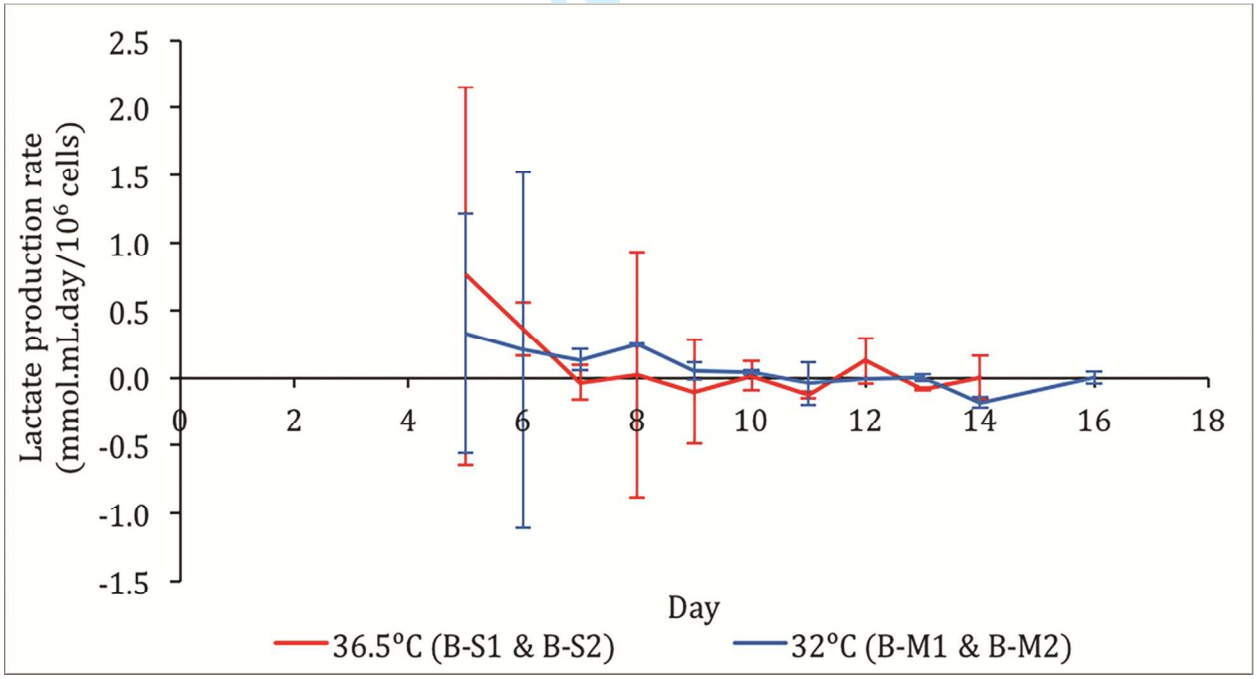

Figure S5: Specific lactate production rate at 36.5°C and 32°C from day 5.

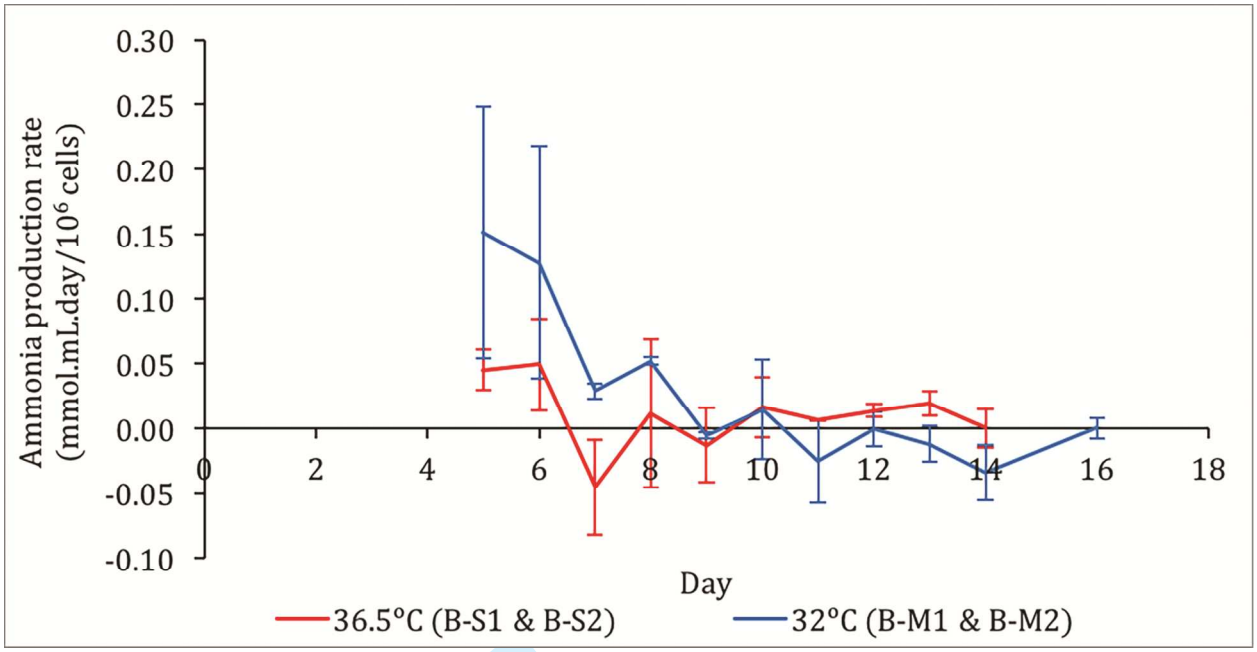

Figure S6: Specific ammonia production rate at 36.5°C and 32°C from day 5.

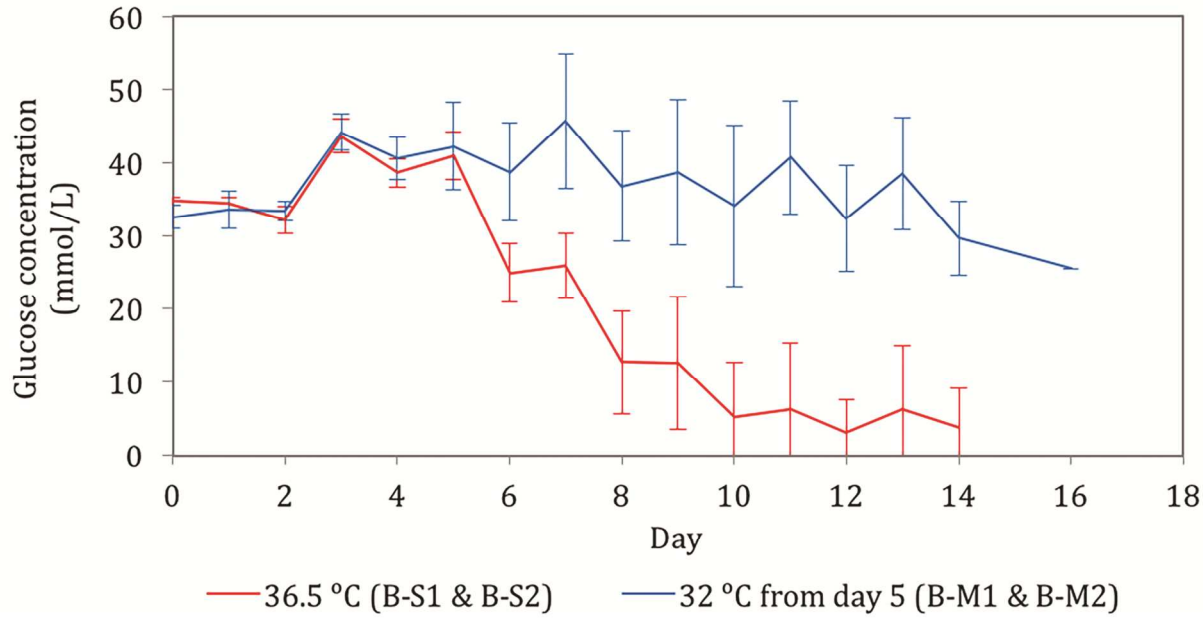

Figure S7: Extracellular glucose concentration at 36.5°C and 32°C from day 5.

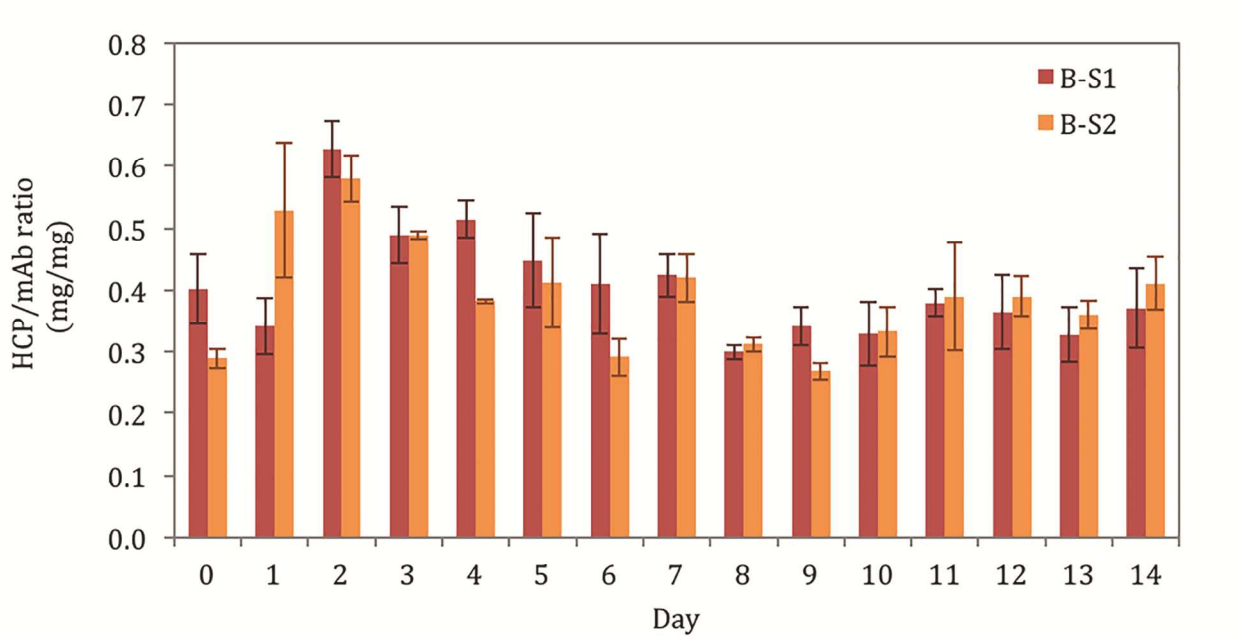

Figure S8: Extracellular HCP/mAb ratio of the control bioreactors (*B-S1* and *B-S2*).

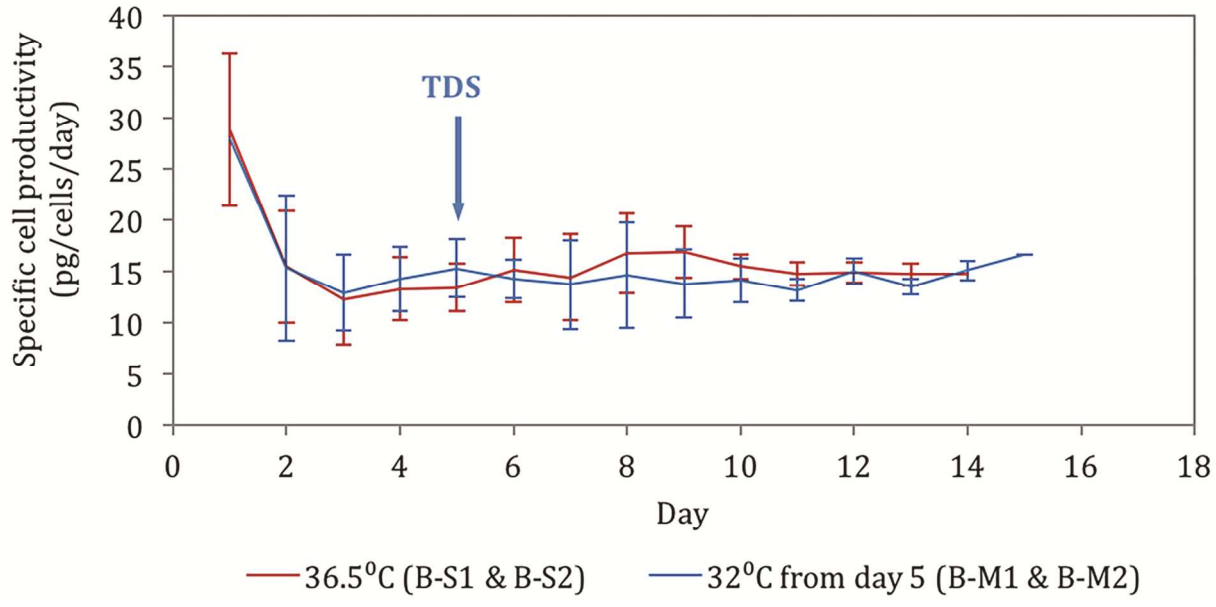

Figure S9: Specific cell productivity (q_{mAb}) at 36.5°C and 32°C from day 5.

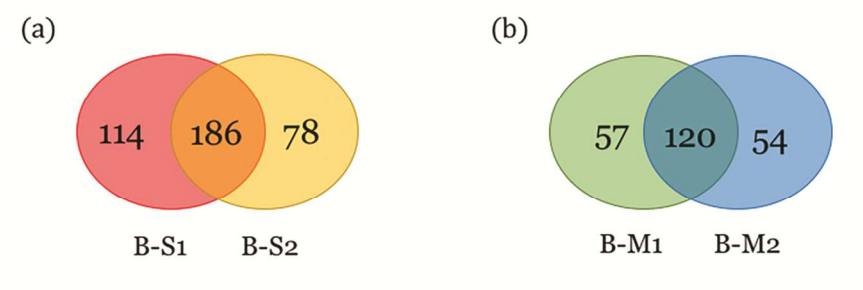

Figure S10: Variation in HCP species at harvest between the bioreactor duplicate at (a) 36.5°C and (b) 32°C from day 5.